Thin Nematic Films on Liquid Substrates†

U. Delabre,*,‡,§ C. Richard,‡,§ and A. M. Cazabat‡,§

Laboratoire de Physique Statistique de l'ENS, 24 rue Lhomond, 75231 Paris Cedex 05, Université Pierre et Marie Curie, 4 place Jussieu, 75252 Paris Cedex 05

Received: July 15, 2008; Revised Manuscript Received: September 11, 2008

Thin films of cyanobiphenyl liquid crystals (nCB) deposited on water or glycerol have been studied in the nematic temperature range. A common property of the systems is the hybrid anchoring conditions at the film interfaces. The preferred orientation of the nematic director is planar at the liquid interface, and it is homeotropic and somewhat weaker at the air interface. The resulting structure of the film depends on its thickness. Films thicker than 0.5 μm show the usual defects of nematics. Between 0.5 μm and 20−30 nm, complex instability patterns such as stripes, "chevrons", or squares are observed in extended films. Then there is a forbidden range of thickness below in which much thinner structures (usually monolayers and trilayers) are present. The present paper investigates this common behavior in various systems and gives arguments for its analysis.

Introduction

Thin films of nematic liquid crystals (LC) are confined media, and their physical parameters and structures may significantly differ from the ones of the bulk phases.[1−6] Most studies use cells where the LC is enclosed between two solid walls situated a few tens of micrometers apart.[7−9] The situation is different if the film has a free interface, in which case the thickness is not imposed. Films of different thicknesses may coexist, and a forbidden range of thickness has been observed for films deposited on oxidized silicon wafers.[4−6,10,11]

The anchoring of liquid crystals, that is, the orientation of the nematic director at interfaces, has been widely investigated.[7−9,12] The anchoring of the n-cyanobiphenyls (nCB) is known to be homeotropic at the free interface (nematic director normal to the interface) and planar degenerate on amorphous silica, water, or glycerol (director in the plane of the interface). These hybrid conditions cause a distortion of the nematic order in the LC film, which is usually described as follows:

Let us call z the normal at the interface which is a xy plane (Figure 1). For relatively thick films, the two interfaces are independent. Let the director be along x on the substrate. It will rotate inside a xz plane to be along z at the free interface (Figure 1a). Within the one-constant approximation,[13−15] the cost of the elastic distortion per unit area is

$$f_{\text{elastic}} = \frac{K(\pi/2)^2}{2h} \qquad (1)$$

where h is the film thickness and K the common value of the elastic constants. For thinner films, the angles at interfaces differ from their preferred values. In the present case, if θ_i is the effective angle of the director with respect to the normal at interfaces (Figure 1b), the free energy can be written as[16]

$$f = \frac{W_1}{2}\cos^2\theta_1 + \frac{W_2}{2}\sin^2\theta_2 + \frac{K(\theta_1 - \theta_2)^2}{2h} \qquad (2)$$

W_1 and W_2 are the anchoring energies per unit area at the substrate and at the free interface, respectively. Associated characteristic lengths are $L_1 = K/W_1$ and $L_2 = K/W_2$. Such a structure with translational invariance along x and with the director rotating inside a xz plane is referred to as a "distorted nematic".

The cost of elastic distortion is too large for very thin films.[17] Below a threshold thickness $h_C = |L_1 - L_2|$ a second-order anchoring transition is observed: thinner films show a homogeneous orientation imposed by the stronger anchoring.

Extrapolation lengths are of the order of micrometers at the air, water, and glycerol interfaces with the anchoring being weaker at the free interface ($L_2 > L_1$).[18] The values of anchoring energy on silica are quite scattered in the literature, but it is accepted that it is weaker than the one on air ($L_2 < L_1$).[4,19]

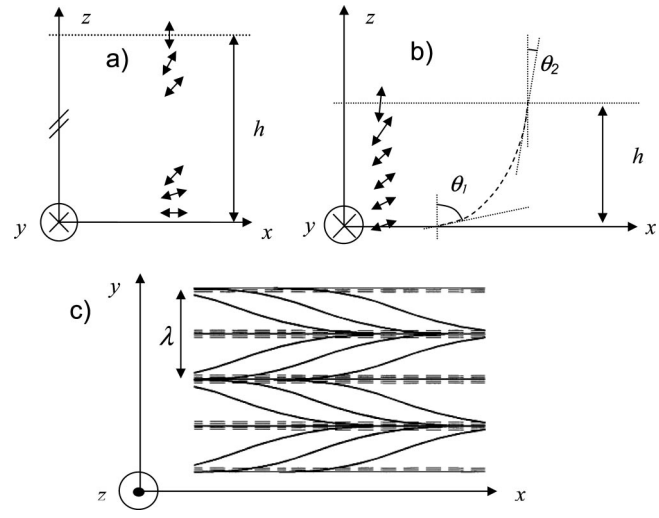

Figure 1. (a) Sketch of a thick film structure: the director is along the easy axis at each interface. (b) Sketch of a thin film structure; the director deviates from the easy direction at each interface. (c) Horizontal projection of the director field in stripes (from Sparavigna et al.[27]).

* To whom correspondence should be addressed.
† Part of "PGG (Pierre-Gilles de Gennes) Memorial Issue".
‡ Laboratoire de Physique Statistique de l'ENS.
§ Université Pierre et Marie Curie.

10.1021/jp8062492 CCC: $40.75 © 2009 American Chemical Society
Published on Web 11/17/2008

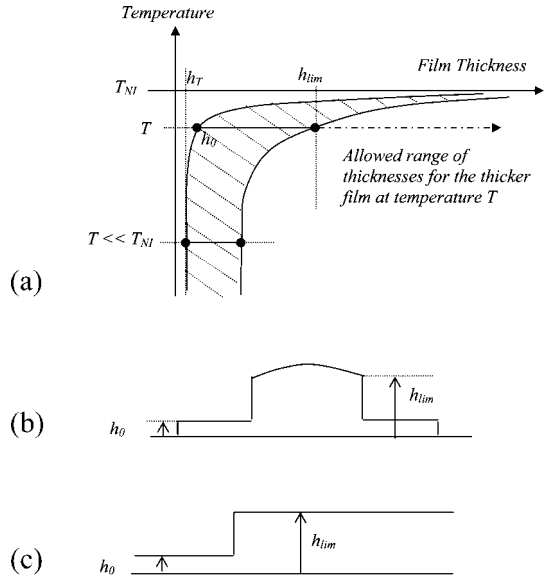

Figure 2. Schematic behavior of thin nematic films with antagonist anchoring at interfaces (adapted from Figure 1, ref 20) On silicon wafers, a thickness discontinuity is observed at the edge of a spreading drop (b).[4,10,11] For spin-coated films and average deposited thickness $h_{average}$, a coexistence is observed between films of thickness h_0 and h_{lim} respectively if $h_0 < h_{average} < h_{lim}$ (2c), and a homogeneous film of thickness $h_{average}$ is observed if $h_{average} > h_{lim}$.[5,6,10] On a liquid substrate, isolated domains of different thicknesses $\geq h_{lim}$ may coexist with the film of thickness h_0. It is accepted[20−25] that all these domains are in metastable equilibrium, except those of thickness h_{lim}, which are in full equilibrium with the film of thickness h_0.

This leads to the following picture:

– on oxidized silicon wafers, the film is distorted above h_C and homeotropic below.

– on water and glycerol, the film is distorted above h_C and planar below.

– except if the two anchoring energies are very close, h_C is less than micrometer but comparable. The specific case $L_1 \cong L_2$, that is, $h_C \ll$ micrometer, should be exceptional.

– As the anchoring transition is second-order, nothing specific is expected when the film thickness crosses value h_C.

Experiments performed in the bulk nematic range of temperatures provide an unexpected landscape, summarized in Figure 2, which analysis is still under debate:

– On oxidized silicon wafers, a thickness discontinuity is observed for both 5CB[4−6,10,11] and 6CB,[20] and on both smooth[5,6,10,11,20] or obliquely evaporated[4] silica. This has been interpreted assuming that the thicker film (thickness h_{lim}) is a distorted nematic ($h_{lim} > h_C$). It coexists with a thinner film (thickness h_0) whose structure is different (see Figure 2a).[4−6,10,11,20] Close to the bulk nematic−isotropic (NI) transition, both films are relatively thick, and the thinner film might be isotropic.[6] Far below the transition, $h_{lim} \approx 20-30$ nm, and the thinner film is a well defined trilayer $h_0 = h_T$.

– far below the NI transition, the behavior of nCB nematic films on liquids (5CB/glycerol, 6CB/glycerol, 6CB/water,[20] 8CB/glycerol, 8CB/water [present study]) is qualitatively similar to the one on silica. Whatever the system, $h_{lim} \approx 20 - 30$ nm. On water, the thinner film is a trilayer ($h_0 = h_T$) both for 8CB[21−24] and 6CB.[25] On glycerol, the precise structure of the thinner film is not known, but thickness h_0 is still in the molecular range.

– On the same nematic nCB/liquid systems, instability patterns are present for $h_{lim} \leq h \leq h_{max}$, with $h_{max} \approx 0.5-0.6$ μm,[20] the wavelengths being much larger than the film thickness. Available models consider azimuthal perturbations (twist) of

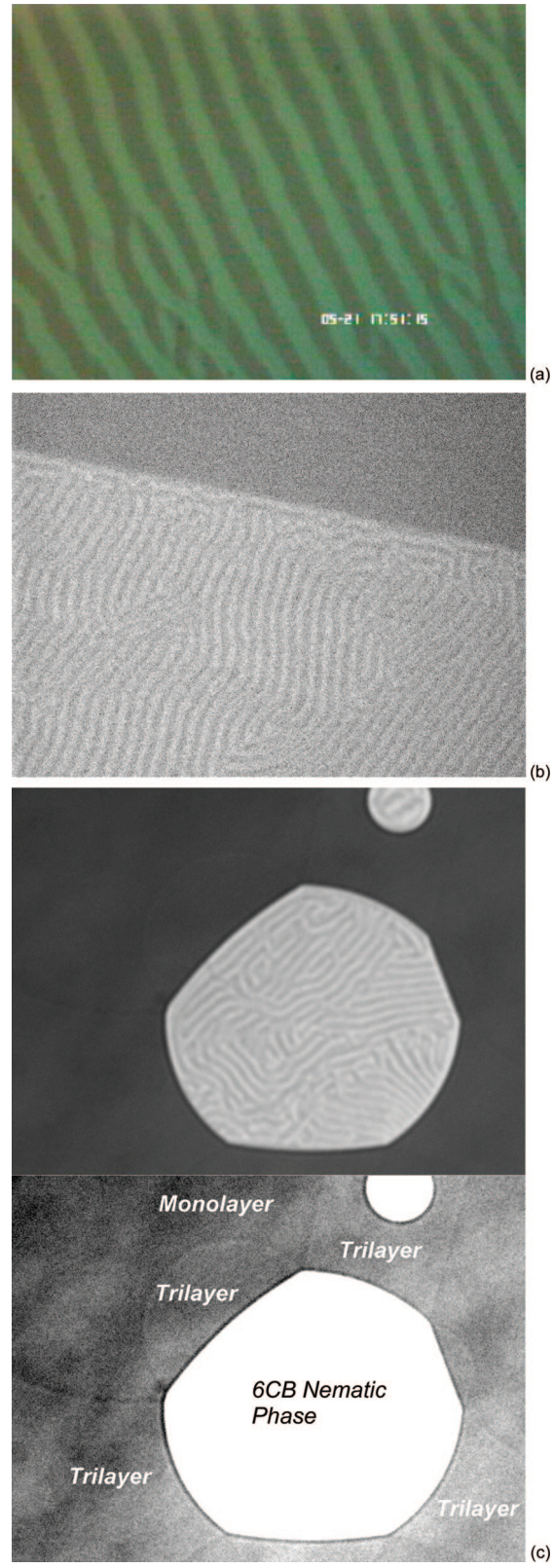

Figure 3. Stripe patterns of the nematic 8CB on glycerol at $T = 35$ °C and 6CB on water at $T = 22$ °C. (a) Stripes of 8 CB on glycerol with $\lambda \sim 50$ μm. Size of image: 630 μm × 475 μm. (b) Stripes of 8CB on glycerol and a film boundary at $h = h_{lim} \approx 20$ nm, $\lambda \sim 2$ μm. Size of image 52 μm × 70 μm. The thinner film in the upper part of the figure is probably a trilayer (≈4 nm thick), but the structure of these films on glycerol has not yet been precisely investigated. (c) Top: striped domain of 6CB on water at $T = 22$ °C. Bottom: same picture but enhanced contrast reveals trilayer films which coexist with the nematic phase. Ahead of the trilayers, the continuous phase is a monolayer.[21−25]

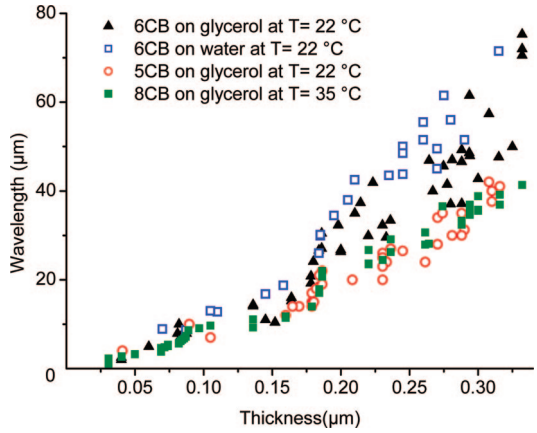

Figure 4. Wavelength (μm) versus thickness (μm) for various compounds. (▲) 6CB on glycerol, (□) 6CB on water, (○) 5CB on glycerol, (■) 8CB on glycerol at $T = 35$ °C. While 5CB and 8CB are at the bottom limit of the nematic phase, 6CB is in the middle.

the "distorted nematic" structure, see Figure 1c.[26−28] Perturbations of homogeneous structures (homeotropic or planar) do not lead to long wavelengths.[29]

Therefore, films as thin as 20−30 nm are distorted, while $h_C = L_2 - L_1$ is at least ten times larger. As previously quoted,[20] eqs 1 and 2, from which the relation $h_C = |L_1 - L_2|$ results, are written in a continuous approximation and do not include van der Waals interaction. However, the continuous approximation is not expected to be drastically wrong in this range of thickness, and the van der Waals contribution becomes negligible above 40 nm.[20]

The present paper proposes an alternative analysis of the results. The procedure is to accumulate data on various systems in order to exclude explanations based on implausible assumptions, that is, very specific values for anchoring energies and elastic constants.[26] Previous results[20] with 5CB and 6CB films on water and glycerol are implemented by an explorative investigation of the structure of instability patterns. New experiments with 8CB on water and glycerol are also performed.

Materials and Methods

The nCB liquid crystals are purchased from Sigma-Aldrich and used as received. The bulk transition temperatures are[15]

$$T_{\text{solid-nematic}} = T_{\text{SN}} = 24\ ^\circ\text{C for 5CB, } 14.5\ ^\circ\text{C for 6CB}$$

$$T_{\text{solid-smectic}} = T_{\text{SSm}} = 21.5\ ^\circ\text{C for 8CB}$$

$$T_{\text{smectic-nematic}} = T_{\text{SmN}} = 33.5\ ^\circ\text{C for 8CB}$$

$$T_{\text{nematic-isotropic}} = T_{\text{NI}} = 35.3\ ^\circ\text{C for 5CB, } 29\ ^\circ\text{C for 6CB, } 40.5\ ^\circ\text{C for 8CB}$$

5CB and 6CB have been studied at room temperature 22 ± 1 °C, far from the NI transitions. 8CB has been studied both at room temperature (in the smectic range) and between 34 and 40 °C (in the nematic range). Surface induced melting is the rule for the nCB,[30] which means that we do not have to consider the occurrence of a SN or SSm transition.

Pure water (18.2 MΩ·cm) and glycerol from Sigma-Aldrich are used as liquid substrates in common Petri dishes. Samples with glycerol must be kept in closed boxes with desiccant in order to avoid uptaking atmospheric water.

Films are obtained by the deposition of drops of solutions of the nCB in hexane. After complete evaporation of the solvent, some local rearrangements including domain coalescence take place during 15−20 mn, and then the films evolve much more slowly over days. While 6CB and 8CB spread both on water and glycerol, 5CB spreads only on glycerol. On water, small droplets with a finite contact angles are obtained. Glycerol is also more convenient than water if heating is needed, because the larger viscosity avoids convection inside the liquid substrate.

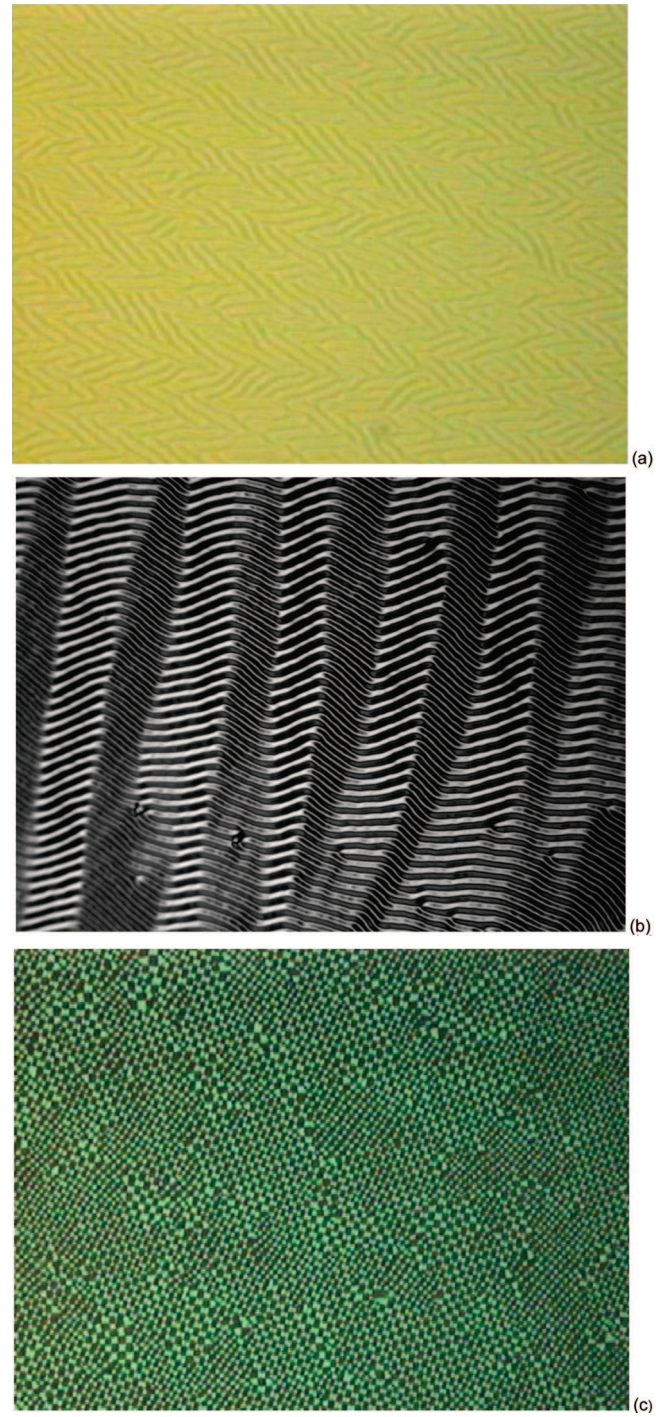

Figure 5. (a) "Chevrons" pattern: 8CB on glycerol at $T = 35$ °C. Size of image 630 μm × 475 μm. (b) Zig-zag pattern: 5CB on glycerol at $T = 22$ °C. Size of image 320 μm × 240 μm (see ref 15, p 203). (c) Square lattice: 6CB on glycerol at $T = 22$ °C. Size of image: 645 μm × 480 μm.

The films are observed under microscope (Polyvar MET-Reichert-Jung) and the images recorded for further analysis. The thickness is estimated using the Newton scale of colors. For the thinnest samples, a high sensitivity black and white camera (CoolSnap-Photometrics) is used. The thickness is estimated by

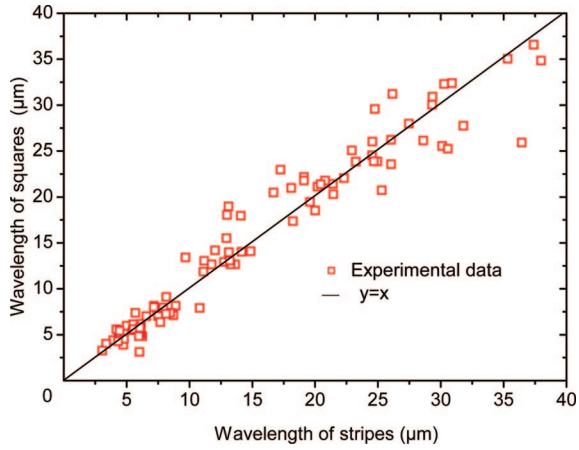

Figure 6. Wavelength of squares versus wavelength of stripes. 6CB on glycerol at $T = 22$ °C.

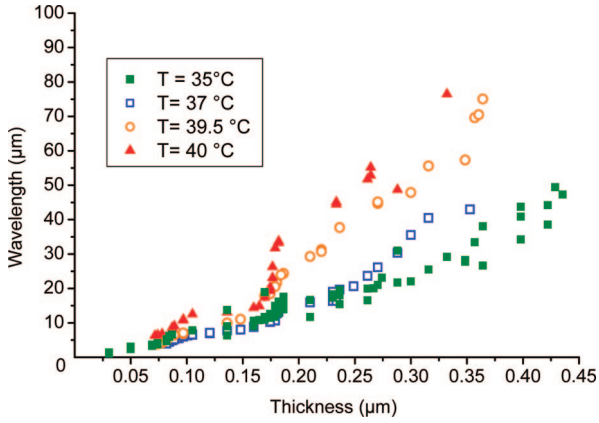

Figure 7. Wavelength versus thickness for the 8CB compound on glycerol at various temperatures. (■) Full squares, $T = 35$ °C; (□) open squares, $T = 37$ °C; (○) open circles, $T = 39.5$ °C; (▲) full triangles, $T = 40$ °C. T_{NI} (8CB) = 40.5 °C. The seemingly oscillatory behavior of the curves is an artifact due to the spectrum of the microscope lamp.

extrapolation of the data for thicker samples and is cross-checked by the intensity scale of the camera.

Experimental Results

Stripe Patterns Far below the NI Transition. Stripe patterns were observed long ago on 5CB films spread on glycerol.[26,27] More recently, a comparative study has been performed on 5CB/glycerol, 6CB/glycerol, and 6CB/water systems.[20] Similar patterns are obtained in the nematic range for 8CB on both water and glycerol (recording is more critical with water, due to easy convection). Figure 3 gives an example of such patterns on glycerol at 35 °C. Note that instability patterns do not occur in 8CB smectic films, where twist is forbidden.[14,15,22−24]

The wavelength λ of the stripes increases with film thickness h, more or less linearly between h_{lim} and typically 0.2−0.3 μm, then steeper, and it diverges at $h_{max} \approx 0.5-0.6$ μm.[20,26,27] Data including the values obtained with 8CB on glycerol at 35 ± 1 °C for $h \leq 0.35$ μm are reported on Figure 4. Strictly speaking, the curves cannot be compared quantitatively because 6CB is closer to the NI transition than the two other compounds. However it is clear that the behavior of the three nCB is qualitatively the same.

The only model available has been proposed by Lavrentovich and Pergamenshchik,[26] and it assumes that stripes result from an azimuthal perturbation of the "distorted nematic" structure (Figure 1c). The complete set of elastic constants which describes splay, bend, and twist deformations. The coupling between them[13−15,26] is required for the analysis. The model agrees on the whole with experimental data for the 5CB/glycerol system, but at the expense of several assumptions:

(1) L_1 and L_2 are very close ($L_1 = 0.76$ μm; $L_2 = 0.86$ μm, $L_2 - L_1 = 0.1$ μm).

(2) Data for $h < 0.15$ μm are excluded from the fit. The authors state that the thickness might significantly change close to the edge of the film, which might cause azimuthal anchoring contributions not included in the analysis.[26,27] As a matter of fact, the model fails for $h \leq 1.5$ $(L_2 - L_1)$.[26]

(3) Ratios K_{13}/K_{11}, K_{24}/K_{11} of the elastic constants[13−15] are very critical to provide the correct shape of the curve $\lambda(h)$ at large h and especially the presence and the position of the wavelength divergence.

These assumptions must be questioned considering the recent[20] and present experiments:

(1) Flat films do exist till $h = h_{lim} \approx 20-30$ nm, even close to the film edge [ref 20 and Figure 3b].

(2, 3) The shape of the curves $\lambda(h)$, and the values of h_{lim} and h_{max} are similar for the 5CB/glycerol, 6CB/water and glycerol, 8CB/glycerol systems, and therefore they are very robust.

To summarize, the robustness of the value of h_{lim} implies that it cannot be always larger than $L_2 - L_1$, and the robustness of both the divergence in wavelength and the corresponding value of h_{max} implies that they cannot depend critically on the ratio of elastic constants. Furthermore, the K_{13} term should be negligible at large thickness because spatial variations of density and order parameter are of minor importance here.[31]

Alternative numerical methods based on a perturbation analysis of the planar state have been developed[27,32] but failed to describe the spectrum of wavelength for stripe patterns.

In fact, parallel stripes are not the sole instability pattern observable in nematic films on water and glycerol. They have been studied because they can be easily treated as azimuthal perturbations of a base state where the director field belongs to the xz plane and is invariant along x (Figure 1). Threshold thickness $h_C = |L_1 - L_2|$ is calculated for this base state, that is, the "distorted nematic". However if stripes are not small perturbations, the base state is no longer relevant to predict any threshold thickness. The presence of patterns with different symmetry supports also this assumption.

Complementary Observations. Patterns with different symmetries easily coexist with stripes. Examples are given in Figure 5.

Such patterns look very similar to the Williams instabilities observed in planar LC samples when an electric field is applied between the walls.[7−9,14,15] Here, the thickness plays the role of the external field. However the wavelengths are at least a hundred times larger than the thickness, and different structures may be observed and even coexist for the same thickness, while for the electro-hydrodynamical instabilities, they are observed for different field strength or frequency.[14,15]

Squared structures are especially interesting because there is no longer a privileged direction. Note that they are mentioned in the review paper by Lavrentovich and Pergamenshchik[28] but without analysis or comment. In Figure 6, the wavelength of squares is plotted versus the one of stripes for the same film thickness. They are close, and this is the strongest support to our previous assumption: instability patterns are not merely small perturbations of the base state represented in Figure 1a,b.

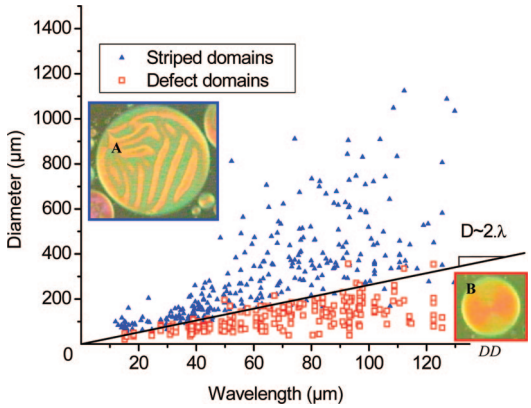

Figure 8. Statistical study of radius versus wavelength and the presence of stripes (extended domains) or a nematic defect (vertical disclination line, small domains). (▲) Full triangles: striped domains. (□) Open squares: defect domains. Domain *DD* (picture B) is the magnified image of one of the little domains visible at the bottom right-hand corner of the main picture A. From the colors, it has the same thickness as the large striped domain but is too small to accommodate stripes.

However, the ingredients of any analysis are still the usual elastic constants, anchoring energies, and characteristic lengths L_1 and L_2. Noticeably, closer to the nematic−isotropic transition, the wavelength increases at a given thickness (see Figure 7) which is associated to the known divergence of K/W.[10,14,15]

Summary and Further Discussion. For all the systems investigated far below the NI transition, the situation is as follows:

– There is a forbidden range for the thickness of nCB nematic films on silica, water, and glycerol.

– The thinner films are molecular structures, a few nanometers thick.

– The minimum thickness of the thicker films is $h_{lim} \approx 20-30$ nm. These films are distorted nematics and their structure on liquid substrates is modified by instability patterns if thickness h is less than 0.6 μm typically. The value of h_{lim} is certainly less than $h_C = |L_1 - L_2|$.

Let us discuss more specifically the case of these "thicker" films ($h_{lim} \leq h \leq h_{max}$).

Data on Liquid Substrates. (1) On liquid substrates, instability patterns provide the clue to explain why films thinner than h_C can be distorted: perturbative analyses[26−28] are not sufficient close to h_{lim}, and therefore the threshold thickness calculated using the in-plane base-state is irrelevant. Even if the conclusion is frustrating, a result possibly useful for further theoretical analysis is the similarity in wavelengths for squares and stripes (Figure 6).

While wavelengths and instability patterns are similar on water and glycerol, this is not the case for the film itself. Flat domains of various sizes and thicknesses coexist on water, while extended films are more easily observed on glycerol. Interesting observations can be made on the 6CB/water system:[25] for a given thickness and therefore a given wavelength, domains smaller than the wavelength cannot accommodate stripes (Figure 8). They show a planar orientation of the director with a disclination line in the center. The orientation has a radial symmetry, which means that either the director is radial, or it is orthoradial everywhere.[14,15] This is also the case at the very edge of striped domains, where a planar configuration is clearly present. Until now, the largest thickness for which such domain edges have been observed is 0.35 μm,[25] which suggests that this might be a lower threshold for h_C. However, further studies are needed to support this conjecture.

(2) Close to the wavelength divergence, stripes become the most probable pattern. Squares and "chevrons" are no longer observed (see the scale in figure 6). Therefore, a perturbative treatment with translational symmetry is probably still relevant. The difficulty with the previous model[26−28] is the sensitivity to the ratios of elastic constants. It is worth noting that what happens around h_{max} is not a mere divergence of wavelength, but the emergence of nonperiodic patterns of nematic defects which should be included in an energy balance.

Data on Solid Substrates. We propose a highly conjectural hypothesis:

Instability patterns are not expected on silica because the homeotropic anchoring (on air) is stronger than the planar one.[4,19,26−29] Moreover, molecules are not free to move on the solid. Therefore, the arguments used on liquid substrates to explain why films thinner than h_C can be distorted seem irrelevant.

However, the question is not about the presence of developed long-wavelength instability, but it is about the ability of the film to relax the elastic energy due to the hybrid anchoring by azimuthal variations of the director. In a somewhat paradoxical way, a random substrate with many strong anchoring defects[33,34] might be more favorable than a homogeneous one with weaker anchoring.

Data might support such an assumption:

– On evaporated silica,[4] the anchoring is planar, nondegenerate. However, a microscopic droplet spreads with radial symmetry, which shows that the anchoring is weak. The measured values of h_{lim} are close to 30 nm.[4]

– On smooth hydrophilic silica, one may expect a large heterogeneity. Strong anchoring defects lead to visible structures on macroscopic spreading drops, and they interact with the flow to generate instability patterns.[35] At the microscopic scale, the measured values of h_{lim} are slightly less than 20 nm.[10]

– On smooth hydrophobic silica, the anchoring is weaker and nothing specific is seen on spreading drops.[11] At the microscopic scale, the measured values of h_{lim} at the edge of these drops are close to 30 nm.[11]

Quite recently, new configurations of thin nematic films have been proposed both theoretically and numerically which involve order reconstruction or what is called a steplike configuration.[36,37] Such configurations have not been observed yet and more controlled experiments are required to answer the question properly.

Conclusion

Instability patterns exist in thin nematic films on liquid substrates and relax the elastic energy by twist deformations down to a film thickness about 20−30 nm. Previous studies of stripe patterns in 5CB and 6CB liquid crystals[20,25] are complemented by new ones using the 8CB in the nematic phase. Noticeably, the dependence of stripes wavelength on temperature is investigated. The accumulation of data and the variety of patterns presented here clearly indicate that the analysis of thin nematic films requires more than a simple perturbation theory of a distorted nematic. In addition, the generality of the results we observe on various compounds and in different situations, rules out previous explanations that require precise values or ratios of elastic and anchoring constants.

A simple projection of this analysis to the solid substrate case is tempting but still highly conjectural.

Acknowledgment. A story of thin films of liquid crystals on oxidized silicon wafers was initiated in the laboratory of

P.G. de Gennes at the Collège de France more than ten years ago. The ellipsometric study of microdroplets or spin-coated films has been achieved with S. Bardon, M. P. Valignat, F. Vandenbrouck, and D. Van Effenterre. C. Poulard has investigated the spontaneous spreading of larger droplets. A.M.C acknowledges Pierre Gilles de Gennes and the members of the laboratory for the warm and keen surrounding there. We gratefully thank G. Guéna who helped a lot in the rebuilding of the "Collège wetting group" at the ENS and J. Meunier for helpful discussions. The present work is partially supported by the Fédération "Dynamique des Systèmes Complexes", headed by M. Ben Amar, and the French CNRS (ANR DYNINSTA-MOBI).

References and Notes

(1) Evans, R.; Marini Bettelo Marconi, U.; Tarazona, P. *J. Chem. Phys.* **1986**, *84*, 2376.
(2) Sheng, P. *Phys. Rev. A* **1982**, *26*, 1610.
(3) Sluckin, T. J.; Ponierwierski, A. *Phys. Rev. Let.* **1985**, *55*, 2907.
(4) Valignat, M. P.; Villette, S.; Li, J.; Barberi, R.; Bartolino, R.; Dubois-Violette, E.; Cazabat, A. M. *Phys. Rev. Lett.* **1996**, *77*, 1994.
(5) Van Effenterre, D.; Ober, R.; Valignat, M. P.; Cazabat, A. M. *Phys. Rev. Lett.* **2001**, *87*, 125701.
(6) (a) Van Effenterre, D. Ph.D. Thesis, University Pierre et Marie Curie, Paris, France, 2002. (b) Van Effenterre, D.; Valignat, M. P.; Roux, D. *Europhys. Lett.* **2003**, *64*, 526.
(7) Williams, R. *J. Chem. Phys.* **1963**, *39*, 384.
(8) Orsay Liquid Crystal group. *Mol. Cryst. Liq. Cryst*. **1971**, *12*, 251.
(9) Dubois-Violette, E.; de Gennes, P. G.; Parodi, O. *J. Phys. Paris* **1971**, *32*, 305.
(10) (a) Bardon, S.;R.; Ober, R.; Valignat, M. P.; Cazabat, A. M.; Daillant, J. *Phys. Rev. E* **1999**, 59–6. (b) Vandenbrouck, F.; Valignat, M. P.; Cazabat, A. M. *Phys. Rev. Lett.* **1999**, *82*, 2693808. (c) Vandenbrouck, F.; Bardon, S.; Valignat, M. P.; Cazabat, A. M. *Phys. Rev. Lett.* **1998**, *81*, 610.
(11) Poulard, C.; Voué, M.; De Coninck, J.; Cazabat, A. M. *Colloids Surf., A* **2006**, *282*, 240.
(12) Jérôme, B. *Rep. Prog. Phys.* **1991**, *54*, 391.
(13) Frank, F. C. *Discuss. Faraday Soc.* **1958**, *25*, 19.
(14) de Gennes, P. G.; Prost, J. *The Physics of Liquid Crystals*, 2nd ed.; Clarendon Press: Oxford, 1993.
(15) Oswald, P.; Pieranski, P.; *Les cristaux liquides*: Gordon and Breach Science Publishers, 2000; Vol. 1.
(16) Rapini, A.; Papoular, M. *J. Phys. (Paris)* **1969**, *30*, C4.
(17) Barbero, G.; Barberi, R. *J. Phys. (Paris)* **1983**, *44*, 609.
(18) Perez, E.; Proust, J. E.; Terminassian-Saraga, L.; Mauer, E. *Colloid Polym. Sci.* **1977**, *255*, 1003.
(19) Ziherl, P. R.; Podgornik, R.; Źeumer, S. *Phys. Rev. Lett.* **2000**, *84*, 1228.
(20) Delabre, U.; Richard, C.; Gúena, G.; Meunier, J.; Cazabat, A. M. *Langmuir* **2008**, *24*, 3998.
(21) de Mul, M. N. G.; Mann, J. A. *Langmuir* **1994**, *10*, 2311.
(22) de Mul, M. N. G.; Mann, J. A. *Langmuir* **1998**, *14*, 2455.
(23) Zou, L.; Wang, J.; Basnet, P.; Mann, E. K. *Phys. Rev. E* **2007**, *76*, 031602.
(24) Läuger, J.; Robertson, C. R.; Frank, C. W.; Fuller, G. G. *Langmuir* **1996**, *12*, 5630.
(25) Delabre, U.; Richard, C.; Meunier, J.; Cazabat, A. M. *Europhys. Lett.*, submitted for publication, 2008.
(26) Lavrentovich, O. D.; Pergamenshchik, V. M. *Phys. Rev. Lett.* **1994**, *73*, 979.
(27) Sparavigna, A.; Lavrentovich, O. D.; Strigazzi, A. *Phys. Rev. E* **1994**, *49*, 1344.
(28) Lavrentovich, O. D.; Pergamenshchik, V. M. *Int. J. Mod. Phys. B* **1995**, *9*, 2389.
(29) Pergamenshchik, V. M. *Phys. Rev. E* **1993**, *47*, 1881.
(30) Barberi, R.; Scaramuzza, N; Formoso, V.; Valignat, M. P.; Bartolino, R.; Cazabat, A. M. *Europhys. Lett.* **1996**, *34*, 349.
(31) Kiselev, A. D. *Phys. Rev. E* **2004**, *69*, 041701.
(32) Krzyzanski, D.; Derfel, G. *Phys. Rev. E* **2001**, *63*, 021702.
(33) Wen, B.; Kim, J.-H.; Yokohama, H.; Rosenblatt, C. *Phys. Rev. E* **2002**, *667*, 041502.
(34) Chiccoli, C.; Lavrentovich, O. D.; Pasini, P.; Zannoni, C. *Phys. Rev. Lett.* **1997**, *72*, 4401.
(35) Poulard, C.; Cazabat, A. M. *Langmuir* **2005**, *21*, 6270.
(36) Sarlah, A.; Zumer, S. *Phys. Rev. E* **1999**, *60*, 1821.
(37) Chiccoli, C.; Pasini, P.; Sarlah, A.; Zannoni, C.; Zumer, S. *Phys. Rev. E* **2003**, *67*, 050703.

JP8062492